Orthogonal Frequency Division Multiplexing With Index Modulation

Ertuğrul Başar, *Member, IEEE*, Ümit Aygölü, *Member, IEEE*, Erdal Panayırcı, *Fellow, IEEE*, and
H. Vincent Poor, *Fellow, IEEE*

Abstract—In this paper, a novel orthogonal frequency division multiplexing (OFDM) scheme, called OFDM with index modulation (OFDM-IM), is proposed for operation over frequency-selective and rapidly time-varying fading channels. In this scheme, the information is conveyed not only by M-ary signal constellations as in classical OFDM, but also by the indices of the subcarriers, which are activated according to the incoming bit stream. Different low complexity transceiver structures based on maximum likelihood detection or log-likelihood ratio calculation are proposed and a theoretical error performance analysis is provided for the new scheme operating under ideal channel conditions. Then, the proposed scheme is adapted to realistic channel conditions such as imperfect channel state information and very high mobility cases by modifying the receiver structure. The approximate pairwise error probability of OFDM-IM is derived under channel estimation errors. For the mobility case, several interference unaware/aware detection methods are proposed for the new scheme. It is shown via computer simulations that the proposed scheme achieves significantly better error performance than classical OFDM due to the information bits carried by the indices of OFDM subcarriers under both ideal and realistic channel conditions.

Index Terms—Frequency selective channels, maximum likelihood (ML) detection, mobility, orthogonal frequency division multiplexing (OFDM), spatial modulation.

I. INTRODUCTION

MULTICARRIER transmission has become a key technology for wideband digital communications in recent years and has been included in many wireless standards to satisfy the increasing demand for high rate communication systems operating on frequency selective fading channels. Orthogonal frequency division multiplexing (OFDM), which can effectively combat the intersymbol symbol interference caused by the frequency selectivity of the wireless channel, has been

the most popular multicarrier transmission technique in wireless communications and has become an integral part of IEEE 802.16 standards, namely Mobile Worldwide Interoperability Microwave Systems for Next-Generation Wireless Communication Systems (WiMAX) and the Long Term Evolution (LTE) project.

In frequency selective fading channels with mobile terminals reaching high vehicular speeds, the subchannel orthogonality is lost due to rapid variation of the wireless channel during the transmission of the OFDM block, and this leads to inter-channel interference (ICI) which affects the system implementation and performance considerably. Consequently, the design of OFDM systems that work effectively under high mobility conditions, is a challenging problem since mobility support is one of the key features of next generation broadband wireless communication systems. Recently, the channel estimation and equalization problems have been comprehensively studied in the literature for high mobility [1], [2].

Multiple-input multiple-output (MIMO) transmission techniques have been also implemented in many practical applications, due to their benefits over single antenna systems. More recently, a novel concept known as spatial modulation (SM), which uses the spatial domain to convey information in addition to the classical signal constellations, has emerged as a promising MIMO transmission technique [3]–[5]. The SM technique has been proposed as an alternative to existing MIMO transmission strategies such as Vertical Bell Laboratories Layered Space-Time (V-BLAST) and space-time coding which are widely used in today's wireless standards. The fundamental principle of SM is an extension of two dimensional signal constellations (such as M-ary phase shift keying (M-PSK) and M-ary quadrature amplitude modulation (M-QAM), where M is the constellation size) to a new third dimension, which is the spatial (antenna) dimension. Therefore, in the SM scheme, the information is conveyed both by the amplitude/phase modulation techniques and by the selection of antenna indices. The SM principle has attracted considerable recent attention from researchers and several different SM-like transmission methods have been proposed and their performance analyses are given under perfect and imperfect channel state information (CSI) in recent works [6]–[12].

The application of the SM principle to the subcarriers of an OFDM system has been proposed in [13]. However, in this scheme, the number of active OFDM subcarriers varies for each OFDM block, and furthermore, a kind of perfect feedforward is assumed from the transmitter to the receiver via the excess subcarriers to explicitly signal the mapping method for the subcarrier index selecting bits. Therefore, this scheme appears to

be quite optimistic in terms of practical implementation. An enhanced subcarrier index modulation OFDM (ESIM-OFDM) scheme has been proposed in [14] which can operate without requiring feedforward signaling from the transmitter to the receiver. However, this scheme requires higher order modulations to reach the same spectral efficiency as that of classical OFDM.

In this paper, taking a different approach from those in [13] and [14], we propose a novel transmission scheme called *OFDM with index modulation (OFDM-IM)* for frequency selective fading channels. In this scheme, information is conveyed not only by M-ary signal constellations as in classical OFDM, but also by the indices of the subcarriers, which are activated according to the incoming information bits. Unlike the scheme of [13], feedforward signaling from transmitter to the receiver is not required in our scheme in order to successfully detect the transmitted information bits. Opposite to the scheme of [14], a general method, by which the number of active subcarriers can be adjusted, and the incoming bits can be systematically mapped to these active subcarriers, is presented in the OFDM-IM scheme. Different mapping and detection techniques are proposed for the new scheme. First, a simple look-up table is implemented to map the incoming information bits to the subcarrier indices and a maximum likelihood (ML) detector is employed at the receiver. Then, in order to cope with the increasing encoder/decoder complexity with the increasing number of information bits transmitted in the spatial domain of the OFDM block, a simple yet effective technique based on combinatorial number theory is used to map the information bits to the antenna indices, and a log-likelihood ratio (LLR) detector is employed at the receiver to determine the most likely active subcarriers as well as corresponding constellation symbols. A theoretical error performance analysis based on pairwise error probability (PEP) calculation is provided for the new scheme operating under ideal channel conditions.

In the second part of the paper, the proposed scheme is investigated under realistic channel conditions. First, an upper bound on the PEP of the proposed scheme is derived under channel estimation errors in which a mismatched ML detector is used for data detection. Second, the proposed scheme is substantially modified to operate under channel conditions in which the mobile terminals can reach high mobility. Considering a special structure of the channel matrix for the high mobility case, three novel ML detection based detectors, which can be classified as interference unaware or aware, are proposed for the OFDM-IM scheme. In addition to these detectors, a minimum mean square error (MMSE) detector, which operates in conjunction with an LLR detector, is proposed. The new scheme detects the higher number of transmitted information bits successfully in the spatial domain.

The main advantages of OFDM-IM over classical OFDM and ESIM-OFDM can be summarized as follows

- The proposed scheme benefits from the frequency selectivity of the channel by exploiting subcarrier indices as a source of information. Therefore, the error performance of the OFDM-IM scheme is significantly better than that of classical OFDM due to the higher diversity orders attained for the bits transmitted in the spatial domain of the OFDM block mainly provided by the frequency selectivity of the channel. This fact is also validated by computer simulations under ideal and realistic channel conditions.
- Unlike the ESIM-OFDM scheme, in which the number of active subcarriers is fixed, the OFDM-IM scheme provides an interesting trade-off between complexity, spectral efficiency and performance by the change of the number of active subcarriers. Furthermore, in some cases, the spectral efficiency of the OFDM-IM scheme can exceed that of classical OFDM without increasing the size of the signal constellation by properly choosing the number of active subcarriers.

The rest of the paper can be summarized as follows. In Section II, the system model of OFDM-IM is presented. In Section III, we propose different implementation approaches for OFDM-IM. The theoretical error performance of OFDM-IM is investigated in Section IV. In Section V, we present new detection methods for the OFDM-IM scheme operating under realistic channel conditions. Computer simulation results are given in Section VI. Finally, Section VII concludes the paper.[1]

II. SYSTEM MODEL OF OFDM-IM

Let us first consider an OFDM-IM scheme operating over a frequency-selective Rayleigh fading channel. A total of m information bits enter the OFDM-IM transmitter for the transmission of each OFDM block. These m bits are then split into g groups each containing p bits, i.e., $m = pg$. Each group of p-bits is mapped to an *OFDM subblock* of length n, where $n = N/g$ and N is the number of OFDM subcarriers, i.e., the size of the fast Fourier transform (FFT). Unlike classical OFDM, this mapping operation is not only performed by means of the modulated symbols, but also by the indices of the subcarriers. Inspired by the SM concept, additional information bits are transmitted by a subset of the OFDM subcarrier indices. For each subblock, only k out of n available indices are employed for this purpose and they are determined by a selection procedure from a predefined set of active indices, based on the first p_1 bits of the incoming p-bit sequence. This selection procedure is implemented by using two different mapping techniques in the proposed scheme. First, a simple look-up table, which provides active indices for corresponding bits, is considered for mapping operation. However, for larger numbers of information bits transmitted in the index domain of the OFDM block, the use of a look-up table becomes infeasible; therefore, a simple and effective technique based on combinatorial number theory is used to map the information bits to the subcarrier indices. Further details can be found in Section III. We set the symbols cor-

---

[1]*Notation*: Bold, lowercase and capital letters are used for column vectors and matrices, respectively. $(\cdot)^T$ and $(\cdot)^H$ denote transposition and Hermitian transposition, respectively. $\det(\mathbf{A})$ and $\text{rank}(\mathbf{A})$ denote the determinant and rank of $\mathbf{A}$, respectively. $\lambda_i(\mathbf{A})$ is the ith eigenvalue of $\mathbf{A}$, where $\lambda_1(\mathbf{A})$ is the largest eigenvalue. $\tilde{\mathbf{A}} = \mathbf{A}(a : b, c : d)$ is a submatrix of $\mathbf{A}$ with dimensions $(b - a + 1) \times (d - c + 1)$, where $\tilde{\mathbf{A}}$ is composed of the rows and columns of $\mathbf{A}$ with indices $a, a + 1, \ldots, b$ and $c, c + 1, \ldots, d$, respectively. $\mathbf{I}_{N \times N}$ and $\mathbf{0}_{N_1 \times N_2}$ are the identity and zero matrices with dimensions $N \times N$ and $N_1 \times N_2$, respectively. $\| \cdot \|_F$ stands for the Frobenius norm. The probability of an event is denoted by $P(\cdot)$ and $E\{\cdot\}$ stands for expectation. The probability density function (p.d.f.) of a random vector $\mathbf{x}$ is denoted by $f(\mathbf{x})$. $X \sim \mathcal{CN}(0, \sigma_X^2)$ represents the distribution of a circularly symmetric complex Gaussian r.v. X with variance σ_X^2. $Q(\cdot)$ denotes the tail probability of the standard Gaussian distribution. $C(n, k)$ denotes the binomial coefficient and $\lfloor \cdot \rfloor$ is the floor function. $\mathcal{S}$ denotes the complex signal constellation of size M.
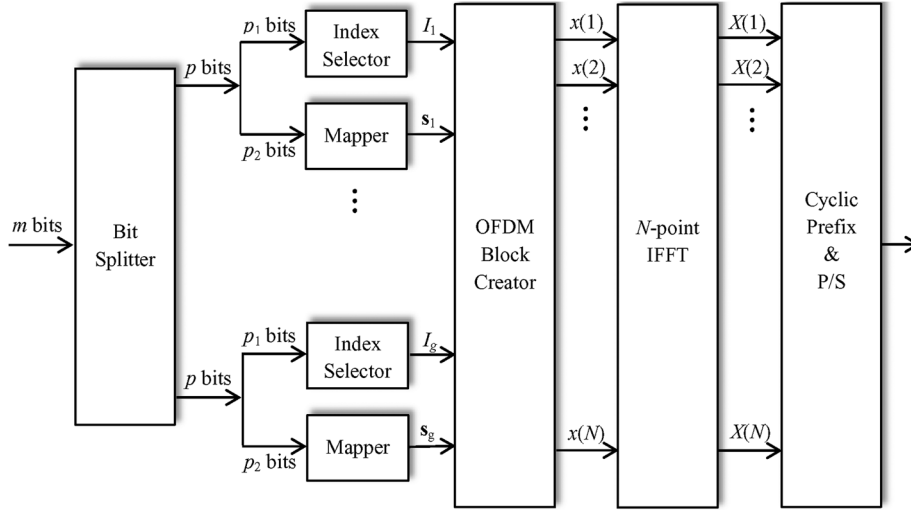
Fig. 1. Block diagram of the OFDM-IM transmitter.

responding to the inactive subcarriers to zero, and therefore, we do not transmit data with them. The remaining $p_2 = k \log_2 M$ bits of this sequence are mapped onto the M-ary signal constellation to determine the data symbols that modulate the subcarriers having active indices; therefore, we have $p = p_1 + p_2$. In other words, in the OFDM-IM scheme, the information is conveyed by both of the M-ary constellation symbols and the indices of the subcarriers that are modulated by these constellation symbols. Due to the fact that we do not use all of the available subcarriers, we compensate for the loss in the total number of transmitted bits by transmitting additional bits in the index domain of the OFDM block.

The block diagram of the OFDM-IM transmitter is given in Fig. 1. For each subblock β, the incoming p_1 bits are transferred to the index selector, which chooses k active indices out of n available indices, where the selected indices are given by

$$I_\beta = \{i_{\beta,1}, \ldots, i_{\beta,k}\} \qquad (1)$$

where $i_{\beta,\gamma} \in [1, \ldots, n]$ for $\beta = 1, \ldots, g$ and $\gamma = 1, \ldots, k$. Therefore, for the total number of information bits carried by the positions of the active indices in the OFDM block, we have

$$m_1 = p_1 g = \lfloor \log_2 \left(C(n,k) \right) \rfloor g. \qquad (2)$$

In other words, I_β has $c = 2^{p_1}$ possible realizations. On the other hand, the total number of information bits carried by the M-ary signal constellation symbols is given by

$$m_2 = p_2 g = k \left(\log_2(M) \right) g \qquad (3)$$

since the total number of active subcarriers is $K = kg$ in our scheme. Consequently, a total of $m = m_1 + m_2$ bits are transmitted by a single block of the OFDM-IM scheme. The vector of the modulated symbols at the output of the M-ary mapper (modulator), which carries p_2 bits, is given by

$$\mathbf{s}_\beta = [s_\beta(1) \ \ldots \ s_\beta(k)] \qquad (4)$$

where $s_\beta(\gamma) \in \mathcal{S}, \beta = 1, \ldots, g, \gamma = 1, \ldots, k$. We assume that $E\{\mathbf{s}_\beta \mathbf{s}_\beta^H\} = k$, i.e., the signal constellation is normalized to

have unit average power. The OFDM block creator creates all of the subblocks by taking into account I_β and $\mathbf{s}_\beta$ for all β first and it then forms the $N \times 1$ main OFDM block

$$\mathbf{x}_F = [x(1) \ x(2) \ \cdots \ x(N)]^T \qquad (5)$$

where $x(\alpha) \in \{0, \mathcal{S}\}, \alpha = 1, \ldots, N$, by concatenating these g subblocks. Unlike the classical OFDM, in our scheme $\mathbf{x}_F$ contains some zero terms whose positions carry information.

After this point, the same procedures as those of classical OFDM are applied. The OFDM block is processed by the inverse FFT (IFFT) algorithm:

$$\mathbf{x}_T = \frac{N}{\sqrt{K}} \text{IFFT}\{\mathbf{x}_F\} = \frac{1}{\sqrt{K}} \mathbf{W}_N^H \mathbf{x}_F \qquad (6)$$

where $\mathbf{x}_T$ is the time domain OFDM block, $\mathbf{W}_N$ is the discrete Fourier transform (DFT) matrix with $\mathbf{W}_N^H \mathbf{W}_N = N \mathbf{I}_N$ and the term $N/\sqrt{K}$ is used for the normalization $E\{\mathbf{x}_T^H \mathbf{x}_T\} = N$ (at the receiver, the FFT demodulator employs a normalization factor of $\sqrt{K}/N$). At the output of the IFFT, a cyclic prefix (CP) of length L samples $[X(N-L+1) \ \cdots \ X(N-1) \ X(N)]^T$ is appended to the beginning of the OFDM block. After parallel to serial (P/S) and digital-to-analog conversion, the signal is sent through a frequency-selective Rayleigh fading channel which can be represented by the channel impulse response (CIR) coefficients

$$\mathbf{h}_T = [h_T(1) \ \ldots \ h_T(\nu)]^T \qquad (7)$$

where $h_T(\sigma), \sigma = 1, \ldots, \nu$ are circularly symmetric complex Gaussian random variables with the $\mathcal{CN}\left(0, \frac{1}{\nu}\right)$ distribution. Assuming that the channel remains constant during the transmission of an OFDM block and the CP length L is larger than ν, the equivalent frequency domain input-output relationship of the OFDM scheme is given by

$$y_F(\alpha) = x(\alpha) h_F(\alpha) + w_F(\alpha), \quad \alpha = 1, \ldots, N \qquad (8)$$

where $y_F(\alpha)$, $h_F(\alpha)$ and $w_F(\alpha)$ are the received signals, the channel fading coefficients and the noise samples in the frequency domain, whose vector presentations are given as $\mathbf{y}_F$, $\mathbf{h}_F$

and $\mathbf{w}_F$, respectively. The distributions of $h_F(\alpha)$ and $w_F(\alpha)$ are $\mathcal{CN}(0,1)$ and $\mathcal{CN}(0, N_{0,F})$, respectively, where $N_{0,F}$ is the noise variance in the frequency domain, which is related by the noise variance in the time domain by

$$N_{0,F} = \left(\frac{K}{N}\right) N_{0,T}. \quad (9)$$

We define the signal-to-noise ratio (SNR) as $\rho = E_b/N_{0,T}$ where $E_b = (N + L)/m$ is the average transmitted energy per bit. The spectral efficiency of the OFDM-IM scheme is given by $m/(N + L)$ [bits/s/Hz].

The receiver's task is to detect the indices of the active subcarriers and the corresponding information symbols by processing $y_F(\alpha)$, $\alpha = 1, \ldots, N$. Unlike classical OFDM, a simple ML decision on $x(\alpha)$ is not sufficient based on $y_F(\alpha)$ only in our scheme due to the index information carried by the OFDM-IM subblocks. In the following, we investigate two different types of detection algorithms for the OFDM-IM scheme:

1) ML Detector: The ML detector considers all possible subblock realizations by searching for all possible subcarrier index combinations and the signal constellation points in order to make a joint decision on the active indices and the constellation symbols for each subblock by minimizing the following metric:

$$(\hat{I}_\beta, \hat{\mathbf{s}}_\beta) = \arg \min_{I_\beta, \mathbf{s}_\beta} \sum_{\gamma=1}^{k} \left| y_F^\beta(i_{\beta,\gamma}) - h_F^\beta(i_{\beta,\gamma}) s_\beta(\gamma) \right|^2 \quad (10)$$

where $y_F^\beta(\xi)$ and $h_F^\beta(\xi)$ for $\xi = 1, \ldots, n$ are the received signals and the corresponding fading coefficients for the subblock β, i.e., $y_F^\beta(\xi) = y_F(n(\beta - 1) + \xi)$, $h_F^\beta(\xi) = h_F(n(\beta - 1) + \xi)$, respectively. It can be easily shown that the total computational complexity of the ML detector in (10), in terms of complex multiplications, is $\sim \mathcal{O}(cM^k)$ per subblock since I_β and $\mathbf{s}_\beta$ have c and M^k different realizations, respectively. Therefore, this ML detector becomes impractical for larger values of c and k due to its exponentially growing decoding complexity.

2) Log-Likelihood Ratio (LLR) Detector: The LLR detector of the OFDM-IM scheme provides the logarithm of the ratio of *a posteriori* probabilities of the frequency domain symbols by considering the fact that their values can be either non-zero or zero. This ratio, which is given below, gives information on the active status of the corresponding index for $\alpha = 1, \ldots, N$:

$$\lambda(\alpha) = \ln \frac{\sum_{\chi=1}^{M} P\left(x(\alpha) = s_\chi \mid y_F(\alpha)\right)}{P\left(x(\alpha) = 0 \mid y_F(\alpha)\right)} \quad (11)$$

where $s_\chi \in \mathcal{S}$. In other words, a larger $\lambda(\alpha)$ value means it is more probable that index α is selected by the index selector at the transmitter, i.e., it is active. Using Bayes' formula and considering that $\sum_{\chi=1}^{M} p(x(\alpha) = s_\chi) = k/n$ and $p(x(\alpha) = 0) = (n - k)/n$, (11) can be expressed as

$$\lambda(\alpha) = \ln(k) - \ln(n - k) + \frac{|y_F(\alpha)|^2}{N_{0,F}}$$

$$+ \ln\left(\sum_{\chi=1}^{M} \exp\left(-\frac{1}{N_{0,F}} |y_F(\alpha) - h_F(\alpha)s_\chi|^2\right)\right). \quad (12)$$

The computational complexity of the LLR detector in (12), in terms of complex multiplications, is $\sim \mathcal{O}(M)$ per subcarrier,

which is the same as that of the classical OFDM detector. In order to prevent numerical overflow, the Jacobian logarithm [15] can be used in (12). As an example, for $k = n/2$ and binary-phase shift keying (BPSK) modulation, (12) simplifies to

$$\lambda(\alpha) = \max(a, b) + \ln\left(1 + \exp\left(-|b - a|\right)\right) + \frac{|y_F(\alpha)|^2}{N_{0,F}} \quad (13)$$

where $a - |y_F(\alpha) - h_F(\alpha)|^2/N_{0,F}$ and $b = -|y_F(\alpha) + h_F(\alpha)|^2/N_{0,F}$.

For higher order modulations, to prevent numerical overflow we use the identity $\ln(e^{a_1} + e^{a_2} + \cdots + e^{a_M}) = f_{max}(f_{max}(\ldots f_{max}(f_{max}(a_1, a_2), a_3), \ldots), a_M)$, where $f_{max}(a, b) = \ln(e^{a_1} + e^{a_2}) = \max(a_1, a_2) + \ln(1 + e^{-|a_1 - a_2|})$. After calculation of the N LLR values, for each subblock, the receiver decides on k active indices out of them having maximum LLR values. This detector is classified as near-ML since the receiver does not know the possible values of I_β. Although this is a desired feature for higher values of n and k, the detector may decide on a catastrophic set of active indices which is not included in I_β since $C(n, k) > c$ for $k > 1$, and $C(n, k) - c$ index combinations are unused at the transmitter.

After detection of the active indices by one of the detectors presented above, the information is passed to the "index demapper", at the receiver which performs the opposite action of the "index selector" block given in Fig. 1, to provide an estimate of the index-selecting p_1 bits. Demodulation of the constellation symbols is straightforward once the active indices are determined.

III. IMPLEMENTATION OF THE OFDM-IM SCHEME

In this subsection, we focus on the index selector and index demapper blocks and provide different implementations of them. As stated in Section II, the index selector block maps the incoming bits to a combination of active indices out of $C(n, k)$ possible candidates, and the task of the index demapper is to provide an estimate of these bits by processing the detected active indices provided by either the ML or LLR OFDM-IM detector.

It is worth mentioning that the OFDM-IM scheme can be implemented without using a bit splitter at the beginning, i.e., by using a single group $(g = 1)$ which results in $n = N$. However, in this case, $C(n, k)$ can take very large values which make the implementation of the overall system difficult. Therefore, instead of dealing with a single OFDM block with higher dimensions, we split this block into smaller subblocks to ease the index selection and detection processes at the transmitter and receiver sides, respectively. The following mappers are proposed for the new scheme:

1) Look-Up Table Method: In this mapping method, a look-up table of size c is created to use at both transmitter and receiver sides. At the transmitter, the look-up table provides the corresponding indices for the incoming p_1 bits for each subblock, and it performs the opposite operation at the receiver. A look-up table example is presented in Table I for $n = 4$, $k = 2$, and $c = 4$, where $s_\chi, s_\zeta \in \mathcal{S}$. Since $C(4, 2) = 6$, two combinations out of six are discarded. Although a very efficient and simple method for smaller c values, this mapping method

TABLE I
A LOOK-UP TABLE EXAMPLE FOR $n = 4$, $k = 2$ AND $p_1 = 2$

Bits	Indices	subblocks
$[0\ 0]$	$\{1,2\}$	$\begin{bmatrix} s_\chi & s_\zeta & 0 & 0 \end{bmatrix}^T$
$[0\ 1]$	$\{2,3\}$	$\begin{bmatrix} 0 & s_\chi & s_\zeta & 0 \end{bmatrix}^T$
$[1\ 0]$	$\{3,4\}$	$\begin{bmatrix} 0 & 0 & s_\chi & s_\zeta \end{bmatrix}^T$
$[1\ 1]$	$\{1,4\}$	$\begin{bmatrix} s_\chi & 0 & 0 & s_\zeta \end{bmatrix}^T$

is not feasible for higher values of n and k due to the size of the table. We employ this method with the ML detector since the receiver has to know the set of possible indices for ML decoding, i.e., it requires a look-up table. On the other hand, a look-up table cannot be used with the LLR detector presented in Section II since the receiver cannot decide on active indices if the detected indices do not exist in the table.

We give the following remark regarding the implementation of the OFDM-IM scheme with a reduced-complexity ML decoding.

Remark: The exponentially growing decoding complexity of the actual ML decoder can be reduced by using a special LLR detector that operates in conjunction with a look-up table. Let us denote the set of possible active indices by $\mathcal{I} = \{I_\beta^1, \ldots, I_\beta^c\}$ for which $I_\beta^\omega \in \mathcal{I}$, where $I_\beta^\omega = \{i_{\beta,1}^\omega, \ldots, i_{\beta,k}^\omega\}$ for $\omega = 1, \ldots, c$. As an example, for the look-up table given in Table I, we have $I_\beta^1 = \{1,2\}$, $I_\beta^2 = \{2,3\}$, $I_\beta^3 = \{3,4\}$, $I_\beta^4 = \{1,4\}$. After the calculation of all LLR values using (12), for each subblock β, the receiver can calculate the following c LLR sums for all possible set of active indices using the corresponding look-up table as

$$d_\beta^\omega = \sum_{\gamma=1}^{k} \lambda \left(n(\beta - 1) + i_{\beta,\gamma}^\omega \right) \qquad (14)$$

for $w = 1, \ldots, c$. Considering Table I, for the first subblock ($\beta = 1$) we have $d_\beta^1 = \lambda(1) + \lambda(2)$, $d_\beta^2 = \lambda(2) + \lambda(3)$, $d_\beta^3 = \lambda(3) + \lambda(4)$, and $d_\beta^4 = \lambda(1) + \lambda(4)$. After calculation of c LLR sums for each subblock, the receiver makes a decision on the set of active indices by choosing the set with the maximum LLR sum, i.e., $\hat{\omega} = \arg\max_\omega d_\beta^\omega$ and obtains the corresponding set of indices, and finally detects the corresponding M-ary constellation symbols. As we will show in the sequel, our simulation results indicate that this reduced-complexity ML decoder exhibits the same BER performance as that of the actual ML detector presented in Section II with higher decoding complexity. On the other hand, for the cases where a look-up table is not feasible, the actual LLR decoder of the OFDM-IM scheme can be implemented by the following method.

2) Combinatorial Method: The combinational number system provides a one-to-one mapping between natural numbers and k-combinations, for all n and k [16], [17], i.e., it maps a natural number to a strictly decreasing sequence $J = \{c_k, \ldots, c_1\}$, where $c_k > \cdots > c_1 \geq 0$. In other words, for fixed n and k, all $Z \in [0, C(n,k) - 1]$ can be presented by a sequence J of length k, which takes elements from the set $\{0, \ldots, n-1\}$ according to the following equation:

$$Z = C(c_k, k) + \cdots + C(c_2, 2) + C(c_1, 1). \qquad (15)$$

As an example, for $n = 8$, $k = 4$, $C(8,4) = 70$, the following J sequences can be calculated:

$$69 = C(7,4) + C(6,3) + C(5,2) + C(4,1) \rightarrow J = \{7,6,5,4\}$$
$$68 = C(7,4) + C(6,3) + C(5,2) + C(3,1) \rightarrow J = \{7,6,5,3\}$$
$$\vdots$$
$$32 = C(6,4) + C(5,3) + C(4,2) + C(1,1) \rightarrow J = \{6,5,4,1\}$$
$$31 = C(6,4) + C(5,3) + C(4,2) + C(0,1) \rightarrow J = \{6,5,4,0\}$$
$$\vdots$$
$$1 = C(4,4) + C(2,3) + C(1,2) + C(0,1) \rightarrow J = \{4,2,1,0\}$$
$$0 = C(3,4) + C(2,3) + C(1,2) + C(0,1) \rightarrow J = \{3,2,1,0\}.$$

The algorithm, which finds the lexicographically ordered J sequences for all n, can be explained as follows: start by choosing the maximal c_k that satisfies $C(c_k, k) \leq Z$, and then choose the maximal c_{k-1} that satisfies $C(c_{k-1}, k-1) \leq Z - C(c_k, k)$ and so on [17]. In our scheme, for each subblock, we first convert the p_1 bits entering the index selector to a decimal number Z, and then feed this decimal number to the combinatorial algorithm to select the active indices as $J + 1$. At the receiver side, after determining active indices, we can easily get back to the decimal number $\hat{Z}$ using (15). This number is then applied to a p_1-bit decimal-to-binary converter. We employ this method with the LLR detector for higher c values to avoid look-up tables. However, it can give a catastrophic result at the exit of the decimal-to-binary converter if $\hat{Z} \geq c$; nevertheless, we use this detector for higher bit-rates.

IV. PERFORMANCE ANALYSIS OF THE OFDM-IM SCHEME

In this section, we analytically evaluate the average bit error probability (ABEP) of the OFDM-IM scheme using the ML decoder with a look-up table.

The channel coefficients in the frequency domain are related to the coefficients in the time domain by

$$\mathbf{h}_F = \mathbf{W}_N \mathbf{h}_T^0 \qquad (16)$$

where $\mathbf{h}_T^0$ is the zero-padded version of the vector $\mathbf{h}_T$ with length N, i.e.,

$$\mathbf{h}_T^0 = [h_T(1) \ \ldots \ h_T(\nu)\ 0\ \ldots\ 0]^T. \qquad (17)$$

It can easily be shown that $h_F(\alpha)$, $\alpha = 1, \ldots, N$, follows the distribution $\mathcal{CN}(0, 1)$, since taking the Fourier transform of a Gaussian vector gives another Gaussian vector. However, the elements of $\mathbf{h}_F$ are no longer uncorrelated. The correlation matrix of $\mathbf{h}_F$ is given as

$$\mathbf{K} = E\left\{ \mathbf{h}_F \mathbf{h}_F^H \right\} = \mathbf{W}_N E\left\{ \mathbf{h}_T^0 \mathbf{h}_T^{0\,H} \right\} \mathbf{W}_N^H = \mathbf{W}_N^H \tilde{\mathbf{I}} \mathbf{W}_N \qquad (18)$$

where

$$\tilde{\mathbf{I}} = \begin{bmatrix} \frac{1}{\nu} \mathbf{I}_{\nu \times \nu} & \mathbf{0}_{\nu \times (N-\nu)} \\ \mathbf{0}_{(N-\nu) \times \nu} & \mathbf{0}_{(N-\nu) \times (N-\nu)} \end{bmatrix}_{N \times N} \qquad (19)$$

is an all-zero matrix except for its first ν diagonal elements which are all equal to $\frac{1}{\nu}$. It should be noted that $\mathbf{K}$ becomes a diagonal matrix if $\nu = N$, which is very unlikely for a practical OFDM scheme. Nevertheless, since $\mathbf{K}$ is a Hermitian Toeplitz

matrix, the PEP events within different subblocks are identical, and it is sufficient to investigate the PEP events within a single subblock to determine the overall system performance. Without loss of generality, we can choose the first subblock, and introduce the following matrix notation for the input-output relationship in the frequency domain:

$$\mathbf{y} = \mathbf{X}\mathbf{h} + \mathbf{w} \quad (20)$$

where $\mathbf{y} = [y_F(1) \cdots y_F(n)]^T$, $\mathbf{X}$ is an $n \times n$ all-zero matrix except for its main diagonal elements denoted by $x(1), \ldots, x(n)$, $\mathbf{h} = [h_F(1) \cdots h_F(n)]^T$ and $\mathbf{w} = [w_F(1) \cdots w_F(n)]^T$. Let us define $\mathbf{K}_n = E\{\mathbf{h}\mathbf{h}^H\}$. In fact, this is an $n \times n$ submatrix centered along the main diagonal of the matrix $\mathbf{K}$. Thus it is valid for all subblocks. If $\mathbf{X}$ is transmitted and it is erroneously detected as $\hat{\mathbf{X}}$, the receiver can make decision errors on both active indices and constellation symbols. The well-known conditional pairwise error probability (CPEP) expression for the model in (20) is given as [18]

$$P(\mathbf{X} \to \hat{\mathbf{X}}|\mathbf{h}) = Q\left(\sqrt{\frac{\delta}{(2N_{0,F})}}\right) \quad (21)$$

where $\delta = \|(\mathbf{X} - \hat{\mathbf{X}})\mathbf{h}\|_F^2 = \mathbf{h}^H \mathbf{A}\mathbf{h}$ and $\mathbf{A} = (\mathbf{X} - \hat{\mathbf{X}})^H(\mathbf{X} - \hat{\mathbf{X}})$. We can approximate $Q(x)$ quite well using [19]

$$Q(x) \cong \frac{1}{12}e^{-x^2/2} + \frac{1}{4}e^{-2x^2/3}. \quad (22)$$

Thus, the unconditional PEP (UPEP) of the OFDM-IM scheme can be obtained by

$$P(\mathbf{X} \to \hat{\mathbf{X}}) \cong E_\mathbf{h}\left\{\frac{1}{12}\exp(-q_1\delta) + \frac{1}{4}\exp(-q_2\delta)\right\} \quad (23)$$

where $q_1 = 1/(4N_{0,F})$ and $q_2 = 1/(3N_{0,F})$. Let $r_1 = \text{rank}(\mathbf{K}_n)$. Since $r_1 < n$ for our scheme, we use the spectral theorem [20] to calculate the expectation above on defining $\mathbf{K}_n = \mathbf{Q}\mathbf{D}\mathbf{Q}^H$ and $\mathbf{h} = \mathbf{Q}\mathbf{u}$, where $E\{\mathbf{u}\mathbf{u}^H\} = \mathbf{D}$ is an $r_1 \times r_1$ diagonal matrix. Considering $\delta = \mathbf{u}^H\mathbf{Q}^H\mathbf{A}\mathbf{Q}\mathbf{u}$ and the p.d.f. of $\mathbf{u}$ given by

$$f(\mathbf{u}) = \frac{\pi^{-r_1}}{\det(\mathbf{D})}\exp(-\mathbf{u}^H\mathbf{D}^{-1}\mathbf{u}) \quad (24)$$

the UPEP can be calculated as

$$P(\mathbf{X} \to \hat{\mathbf{X}})$$
$$\cong \frac{\pi^{-r_1}}{12\det(\mathbf{D})}\int_\mathbf{u}\exp\left(-\mathbf{u}^H[\mathbf{D}^{-1} + q_1\mathbf{Q}^H\mathbf{A}\mathbf{Q}]\mathbf{u}\right)d\mathbf{u}$$
$$+ \frac{\pi^{-r_1}}{4\det(\mathbf{D})}\int_\mathbf{u}\exp\left(-\mathbf{u}^H[\mathbf{D}^{-1} + q_2\mathbf{Q}^H\mathbf{A}\mathbf{Q}]\mathbf{u}\right)d\mathbf{u} \quad (25)$$

$$= \frac{1/12}{\det\left(\mathbf{I}_{r_1} + q_1\mathbf{D}\mathbf{Q}^H\mathbf{A}\mathbf{Q}\right)} + \frac{1/4}{\det\left(\mathbf{I}_{r_1} + q_2\mathbf{D}\mathbf{Q}^H\mathbf{A}\mathbf{Q}\right)} \quad (26)$$

$$= \frac{1/12}{\det(\mathbf{I}_n + q_1\mathbf{Q}\mathbf{D}\mathbf{Q}^H\mathbf{A})} + \frac{1/4}{\det(\mathbf{I}_n + q_2\mathbf{Q}\mathbf{D}\mathbf{Q}^H\mathbf{A})} \quad (27)$$

$$= \frac{1/12}{\det(\mathbf{I}_n + q_1\mathbf{K}_n\mathbf{A})} + \frac{1/4}{\det(\mathbf{I}_n + q_2\mathbf{K}_n\mathbf{A})} \quad (28)$$

$n \setminus \nu$	4	7	10	13	
4	2	2	3	3	←r_1
	0.0598	0.1883	0.0001	0.0005	←δ
8	3	3	3	4	
	0.0002	0.0086	0.0695	0.0001	
16	3	4	5	5	
	0.1209	0.0038	0.00003	0.0037	
32	4	5	6	7	
	0.1013	0.2506	0.2094	0.1065	

where (25) and (26) are related via (24), and (27) is obtained from the identity

$$\det(\mathbf{I}_{r_1} + \mathbf{M}\mathbf{N}) = \det(\mathbf{I}_n + \mathbf{N}\mathbf{M}) \quad (29)$$

where the dimensions of $\mathbf{M}$ and $\mathbf{N}$ are $r_1 \times n$ and $n \times r_1$, respectively. We have the following remarks:

Remark 1 (Diversity Order of the System): Let us define $\mathbf{A}_i = \mathbf{I}_n + q_i\mathbf{K}_n\mathbf{A} = \mathbf{I}_n + q_i\mathbf{B}$ for $i = 1, 2$. Since

$$\det(\mathbf{A}_i) = \prod_{\xi=1}^{n}\lambda_\xi(\mathbf{A}_i) = \prod_{\xi=1}^{r}(1 + q_i\lambda_\xi(\mathbf{B})) \quad (30)$$

where $r = \text{rank}(\mathbf{B})$, for high SNR values ($q_i \gg 1$), we can rewrite (28) as

$$P(\mathbf{X} \to \hat{\mathbf{X}}) \simeq \left(12q_1^r\prod_{\xi=1}^{r}\lambda_\xi(\mathbf{B})\right)^{-1} + \left(4q_2^r\prod_{\xi=1}^{r}\lambda_\xi(\mathbf{B})\right)^{-1}. \quad (31)$$

As seen from this result, the diversity order of the system is determined by r, which is upper bounded according to the rank inequality [20] by $r \le \min\{r_1, r_2\}$, where $r_2 = \text{rank}(\mathbf{A})$. On the other hand we have $\min r_2 = 1$ when the receiver correctly detects all of the active indices and makes a single decision error out of k M-ary symbols. It can be shown that r can take values from the interval $[1, n]$.

Remark 2 (Effects of Varying ν Values): Keeping in mind that the diversity order of the system is determined by the worst case PEP scenario when $r_2 = 1$, we conclude that the distance spectrum of the system improves by increasing the values of r_1, which is a new phenomenon special to the OFDM-IM concept as opposed to classical OFDM. As a secondary factor, considering the inequality $\prod_{t=1}^{r}\lambda_{i_t}(\mathbf{K}_n\mathbf{A}) \le \prod_{t=1}^{r}\lambda_{i_t}(\mathbf{K}_n)\lambda_t(\mathbf{A})$ for the eigenvalues of the products of positive semidefinite Hermitian matrices [21] where $1 \le i_1 < \cdots < i_r \le r$, we also conclude that the UPEP decreases with increasing values of $\delta = \prod_{t=1}^{r_1}\lambda_t(\mathbf{K}_n)$. In Table II, for varying n and ν values, corresponding to the r_1 and δ values, are calculated for $N = 128$, where we assumed that $\lambda_t(\mathbf{K}_n) = 0$ if $\lambda_t(\mathbf{K}_n) < 10^{-4}$. As seen from Table II, r_1 and δ values increase with increasing values of ν, i.e., increasing frequency selectivity of the fading channel. However, although this a factor which improves the PEP distance spectrum of the OFDM-IM scheme, it does not considerably affect the error performance for high SNR values because the worst case PEP event with $r_2 = 1$ dominates the system performance in the high SNR regime. In other words, $\det(\mathbf{A}_i)$, $i = 1, 2$, does not change for different ν values when

$r_2 = 1$. We also observe from Table II that r_1 and δ values also increase with the increasing values of n; nevertheless, it is not possible to make a fair comparison for this case because the spectral efficiency of the system also increases (due to the increasing number of bits transmitted in the index domain) with increasing values of n. On the other hand, we observe from Table II that the effect of the increasing ν values on the error performance can be more explicit for larger n values in the low-to-mid SNR regime due to the larger variation on r_1 values.

Remark 3 (Improving the Diversity Order): To improve the diversity order of the system, we can by-pass the M-ary modulation by setting $p = p_1$ and only transmit data via the indices of the active subcarriers at the expense of reducing the bit rate, since we always guarantee $r_2 \geq 2$ in the absence of the symbol errors.

Remark 4 (Generalization): Although the CPEP expression given in (21) and therefore, the main results presented above are valid for ML detector of the OFDM-IM scheme, as we will show in the sequel, the error performance of the near-ML LLR detector is almost identical as that of the ML detector; therefore, without loss of generality, the presented results can be assumed to be valid for OFDM-IM schemes employing LLR detectors.

After the evaluation of the UPEP from (28), the ABEP of the OFDM-IM can be evaluated by

$$P_b \approx \frac{1}{pn_{\mathbf{X}}} \sum_{\mathbf{X}} \sum_{\hat{\mathbf{X}}} P(\mathbf{X} \to \hat{\mathbf{X}}) e(\mathbf{X}, \hat{\mathbf{X}}) \tag{32}$$

where $n_{\mathbf{X}}$ is the number of the possible realizations of $\mathbf{X}$ and $e(\mathbf{X}, \hat{\mathbf{X}})$ represents the number of bit errors for the corresponding pairwise error event.

V. OFDM-IM UNDER REALISTIC CHANNEL CONDITIONS

In this section, we analyze the OFDM-IM scheme under realistic channel conditions such as imperfect CSI and very high mobility by providing analytical tools to determine the error performance and proposing different implementation techniques.

A. OFDM-IM Under Channel Estimation Errors

In this subsection, we analyze the effects of channel estimation errors on the error performance of the OFDM-IM scheme.

In practical systems, the channel estimator at the receiver provides an estimate of the vector of the channel coefficients $\mathbf{h}$ as [22]

$$\tilde{\mathbf{h}} = \mathbf{h} + \boldsymbol{\epsilon} \tag{33}$$

where $\boldsymbol{\epsilon}$ represents the vector of channel estimation errors which is independent of $\mathbf{h}$, and has the covariance matrix $E\{\boldsymbol{\epsilon}\boldsymbol{\epsilon}^H\} = \sigma_\epsilon^2 \mathbf{I}_n$. In this work, we assume that $N_{0,F}$ and σ_ϵ^2 are related via $Q = N_{0,F}/\sigma_\epsilon^2$, i.e., the power of the estimation error decreases with increasing SNR. Under channel estimation errors, the receiver uses the mismatched ML decoder by processing the received signal vector given by (20) to detect the corresponding data vector as

$$\hat{\mathbf{X}} = \arg \min_{\mathbf{X}} \|\mathbf{y} - \mathbf{X}\tilde{\mathbf{h}}\|^2. \tag{34}$$

In other words, the receiver uses the decision metric of the perfect CSI (P-CSI) case by simply replacing $\mathbf{h}$ by $\tilde{\mathbf{h}}$. For this case, (20) can be rewritten as

$$\mathbf{y} = \mathbf{X}\tilde{\mathbf{h}} + \mathbf{X}(\mathbf{h} - \tilde{\mathbf{h}}) + \mathbf{w} = \mathbf{X}\tilde{\mathbf{h}} + \tilde{\mathbf{w}}, \tag{35}$$

where $\tilde{\mathbf{w}} \triangleq \mathbf{X}(\mathbf{h} - \tilde{\mathbf{h}}) + \mathbf{w} = -\mathbf{X}\boldsymbol{\epsilon} + \mathbf{w}$. Considering (34) and (35), the CPEP of the OFDM-IM scheme can be calculated as follows:

$$
\begin{aligned}
&P(\mathbf{X} \to \hat{\mathbf{X}}|\tilde{\mathbf{h}}) \\
&= P\left(\|\mathbf{y} - \mathbf{X}\tilde{\mathbf{h}}\|^2 > \|\mathbf{y} - \hat{\mathbf{X}}\tilde{\mathbf{h}}\|^2\right) \\
&= P\left(\|\mathbf{X}\tilde{\mathbf{h}}\|^2 - \|\hat{\mathbf{X}}\tilde{\mathbf{h}}\|^2 - 2\Re\left\{\mathbf{y}^H(\mathbf{X} - \hat{\mathbf{X}})\tilde{\mathbf{h}}\right\} > 0\right) \\
&= P\left(-\left\|(\mathbf{X} - \hat{\mathbf{X}})\tilde{\mathbf{h}}\right\|^2 - 2\Re\left\{\tilde{\mathbf{w}}^H(\mathbf{X} - \hat{\mathbf{X}})\tilde{\mathbf{h}}\right\} > 0\right) \\
&= P(D > 0).
\end{aligned} \tag{36}
$$

It can be shown that the decision variable D is Gaussian distributed with

$$E\{D\} = -\left\|(\mathbf{X} - \hat{\mathbf{X}})\tilde{\mathbf{h}}\right\|^2$$

$$Var\{D\} = 2\sigma_\epsilon^2 \left\|\mathbf{X}^H(\mathbf{X} - \hat{\mathbf{X}})\tilde{\mathbf{h}}\right\|^2 + 2N_{0,F}\left\|(\mathbf{X} - \hat{\mathbf{X}})\tilde{\mathbf{h}}\right\|^2$$

which yields the following CPEP expression:

$$
P(\mathbf{X} \to \hat{\mathbf{X}}|\tilde{\mathbf{h}}) \\
= Q\left(\frac{\left\|(\mathbf{X} - \hat{\mathbf{X}})\tilde{\mathbf{h}}\right\|^2}{\sqrt{2\sigma_\epsilon^2\left\|\mathbf{X}^H(\mathbf{X} - \hat{\mathbf{X}})\tilde{\mathbf{h}}\right\|^2 + 2N_{0,F}\left\|(\mathbf{X} - \hat{\mathbf{X}})\tilde{\mathbf{h}}\right\|^2}}\right). \tag{37}
$$

In order to obtain the UPEP, the CPEP expression given in (37) should be averaged over the multivariate complex Gaussian p.d.f. of $\tilde{\mathbf{h}}$ which is given by [23]

$$f(\tilde{\mathbf{h}}) = \frac{\pi^{-n}}{\det(\tilde{\mathbf{K}}_n)} \exp\left(-\tilde{\mathbf{h}}^H \tilde{\mathbf{K}}_n^{-1}\tilde{\mathbf{h}}\right). \tag{38}$$

where $\tilde{\mathbf{K}} = E\{\tilde{\mathbf{h}}\tilde{\mathbf{h}}^H\} = \mathbf{K}_n + \sigma_\epsilon^2 \mathbf{I}_n$ and $\text{rank}(\tilde{\mathbf{K}}) = n$. However, due to the complexity of (37), this operation is not an easy task, therefore, we consider the following upper bound for the CPEP of the OFDM-IM scheme:

$$P(\mathbf{X} \to \hat{\mathbf{X}}|\tilde{\mathbf{h}}) \leq Q\left(\sqrt{\frac{\left\|(\mathbf{X} - \hat{\mathbf{X}})\tilde{\mathbf{h}}\right\|^2}{2\sigma_\epsilon^2 + 2N_{0,F}}}\right) \tag{39}$$

which is obtained by using the inequality

$$\left\|\mathbf{X}^H(\mathbf{X} - \hat{\mathbf{X}})\tilde{\mathbf{h}}\right\|^2 \leq \left\|(\mathbf{X} - \hat{\mathbf{X}})\tilde{\mathbf{h}}\right\|^2 \tag{40}$$

where both inequalities hold if all active subcarrier indices have been correctly detected. In other words, the actual CPEP expression given in (37) simplifies to the CPEP expression given in (39) for the error events corresponding to the erroneous detection of only M-ary symbols in a given subblock

which are chosen from a constant envelope constellation as M-PSK since

$$\left\| \mathbf{X}^H (\mathbf{X} - \hat{\mathbf{X}}) \tilde{\mathbf{h}} \right\|^2 = \sum_{i=1}^{n} \left| x_i (x_i - \hat{x}_i) \tilde{h}_i \right|^2$$

$$\left\| (\mathbf{X} - \hat{\mathbf{X}}) \tilde{\mathbf{h}} \right\|^2 = \sum_{i=1}^{n} \left| (x_i - \hat{x}_i) \tilde{h}_i \right|^2$$

where $\mathbf{X} = \mathrm{diag}([x_1 \ \ldots \ x_n])$, $\hat{\mathbf{X}} = \mathrm{diag}([\hat{x}_1 \ \ldots \ \hat{x}_n])$ and $\tilde{\mathbf{h}} = [\tilde{h}_1 \ \ldots \ \tilde{h}_n]$, and only k out of n x_i's have non-zero values. Using (22) and (38), the UPEP upper bound of the OFDM-IM scheme with channel estimation errors can be calculated as follows:

$$P(\mathbf{X} \to \hat{\mathbf{X}}) \leq \frac{\pi^{-n}}{12 \det(\tilde{\mathbf{K}}_n)} \int_{\tilde{\mathbf{h}}} \exp\left(-\tilde{\mathbf{h}}^H \left[\tilde{\mathbf{K}}_n^{-1} + \tilde{q}_1 \mathbf{A} \right] \tilde{\mathbf{h}} \right) d\tilde{\mathbf{h}}$$

$$+ \frac{\pi^{-n}}{4 \det(\tilde{\mathbf{K}}_n)} \int_{\tilde{\mathbf{h}}} \exp\left(-\tilde{\mathbf{h}}^H \left[\tilde{\mathbf{K}}_n^{-1} + \tilde{q}_2 \mathbf{A} \right] \tilde{\mathbf{h}} \right) d\tilde{\mathbf{h}}$$

$$= \frac{1/12}{\det(\mathbf{I}_n + \tilde{q}_1 \tilde{\mathbf{K}}_n \mathbf{A})} + \frac{1/4}{\det(\mathbf{I}_n + \tilde{q}_2 \tilde{\mathbf{K}}_n \mathbf{A})} \quad (41)$$

where $\tilde{q}_1 = 1/(4\sigma_\epsilon^2 + 4N_{0,F})$, $\tilde{q}_2 = 1/(3\sigma_\epsilon^2 + 3N_{0,F})$ and $\mathbf{A} = (\mathbf{X} - \hat{\mathbf{X}})^H (\mathbf{X} - \hat{\mathbf{X}})$. After calculation of the UPEP, the ABEP of the OFDM-IM can be evaluated by using (32).

In order to obtain a different approximation to the actual UPEP, one can consider the UPEP in the high-SNR regime in which the worst case error events and their multiplicities dominate the error performance. Similar to the P-CSI case, according to (41), the diversity order of the system is determined by $\mathrm{rank}(\tilde{\mathbf{K}}_n \mathbf{A})$, which is upper bounded by $\mathrm{rank}(\mathbf{A}) = 1$, i.e., the system performance is dominated by the error events corresponding to the erroneous detection of only M-ary symbols in a given subblock. Therefore, for this type of error events the inequality given in (39) holds and the actual UPEP can be evaluated by (41), and then the ABEP can be calculated by using (32) considering only the corresponding worst case error events. On the other hand, the calculation of the UPEP for general M-ary signal constellations is left for future work.

B. OFDM-IM Under Very High Mobility

It is well known that OFDM eliminates intersymbol interference and simply uses a one-tap equalizer to compensate for multiplative channel distortion in quasi-static and frequency-selective channels. However, in fading channels with very high mobilities, the time variation of the channel over one OFDM symbol period results in a loss of subchannel orthogonality which leads to ICI. The received signal in the frequency domain can be expressed as [24]

$$\mathbf{y}_F = \mathbf{G}\mathbf{x}_F + \mathbf{w}_F \quad (42)$$

where $\mathbf{G} = \mathbf{W}_N \mathbf{H} \mathbf{W}_N^H$ which $\mathbf{H}$ the equivalent channel matrix in the time domain and $\mathbf{W}_N$ the FFT matrix, and it is no longer diagonal due to the ICI. Unlike the system model given in Section II, we assume that some of the available subcarriers are not allocated for data transmission, i.e., the OFDM block is

padded by zeros. In particular, we assume that the first and last $N_{zp}/2$ elements of the main OFDM block are not used for data transmission, where N_{zp} is the size of the zero padding. Considering that the first and the last $N_{zp}/2$ elements of the main OFDM block have been padded with zeros, we define the meaningful received signal vector, OFDM block and the channel matrix, respectively, as follows: $\tilde{\mathbf{y}}_F = \mathbf{y}_F(\mathcal{J})$, $\tilde{\mathbf{x}}_F = \mathbf{x}_F(\mathcal{J})$, and $\tilde{\mathbf{G}} = \mathbf{G}(\mathcal{J}, \mathcal{J})$, where $\mathcal{J} = \frac{N_{zp}}{2} + 1 : N - \frac{N_{zp}}{2}$.

Due to the structure of the modified channel matrix $\mathbf{G}$ given in (42), different OFDM subblocks interfere with each other, unlike in the model of Section II; therefore, algorithms are required to detect the active indices as well as the corresponding constellation symbols. MMSE equalization can be considered as an efficient solution to the detection problem of (42) because the interference between the different OFDM subblocks can be easily eliminated by MMSE equalization. However, as we will show in the sequel, MMSE detection can diminish the effectiveness of the transmission of the additional bits in the spatial domain by eliminating the effect of the channel matrix completely on the transmitted OFDM block. On the other hand, considering the banded structure of the channel matrix $\mathbf{G}$, different interference unaware or aware detection algorithms can be implemented for the OFDM-IM scheme. In the following, we propose different detection methods for the OFDM-IM scheme under mobility:

1) MMSE Detector: The MMSE detector chooses the matrix $\tilde{\mathbf{G}}^H$ (called the equalizer matrix) that minimizes the cost function $E\{|\tilde{\mathbf{x}}_F - \tilde{\mathbf{G}}^H \tilde{\mathbf{y}}_F|^2\}$. The resulting detection statististic becomes

$$\mathbf{y}_{MMSE} = \tilde{\mathbf{G}}^H \left(\tilde{\mathbf{G}} \tilde{\mathbf{G}}^H + \frac{\mathbf{I}_{N_{av}}}{\rho_F} \right)^{-1} \tilde{\mathbf{y}}_F \quad (43)$$

where $\mathbf{y}_{MMSE}$ is the MMSE equalized signal, ρ_F is the average SNR at the frequency domain, and $N_{av} = N - N_{zp}$ is the number of available subcarriers. After MMSE equalization, which eliminates the ICI caused by the time selective channels with high mobility, one can consider either of the reduced-complexity ML or LLR detectors to determine the active indices and corresponding constellation symbols depending on the system configuration. As an example, for the case of the LLR decoder, (12) can be used for detection with the assumption of $h_F(\alpha) = 1$ for all α due to the effect of the MMSE equalization. For the reduced-complexity ML decoder, the calculated LLR values are used with the look-up table to determine the corresponding LLR sums.

2) Submatrix Detector: This interference unaware detector assumes that $\tilde{\mathbf{G}} \approx \tilde{\mathbf{G}}_{sub}$, where $\tilde{\mathbf{G}}_{sub}$ has the following structure:

$$\tilde{\mathbf{G}}_{sub} = \begin{bmatrix} \tilde{\mathbf{G}}_1 & 0 & \cdots & 0 \\ 0 & \tilde{\mathbf{G}}_2 & & \vdots \\ \vdots & & \ddots & \\ 0 & \cdots & & \tilde{\mathbf{G}}_g \end{bmatrix} \quad (44)$$

where $\tilde{\mathbf{G}}_\beta = \tilde{\mathbf{G}}(n\beta - n + 1 : n\beta, n\beta - n + 1 : n\beta)$ is an $n \times n$ matrix that corresponds to the subblock β, $\beta = 1, \ldots, g$. In other words, this detector does not consider the interference between different subblocks. Therefore, for each subblock, the

receiver makes a joint decision on the active indices and the constellation symbols by minimizing the following metric:

$$\hat{\mathbf{x}}_F^\beta = \arg\min_{\tilde{\mathbf{x}}_F^\beta} \left\| \tilde{\mathbf{y}}_F^\beta - \tilde{\mathbf{G}}_\beta \tilde{\mathbf{x}}_F^\beta \right\|_F^2 \qquad (45)$$

where $\tilde{\mathbf{y}}_F^\beta = \tilde{\mathbf{y}}_F(n\beta - n + 1 : n\beta)$ is the corresponding received signal vector of length n for OFDM-IM subblock $\tilde{\mathbf{x}}_F^\beta = \tilde{\mathbf{x}}_F(n\beta - n + 1 : n\beta)$, which has cM^k different realizations. Therefore, unlike the MMSE detector, the decoding complexity of this detector grows exponentially with increasing values of k.

3) Block Cancellation Detector: The block cancellation detector applies the same procedures as those of the submatrix detector; however, after the detection of $\tilde{\mathbf{x}}_F^\beta$, this detector updates the received signal vector by eliminating the interference of $\tilde{\mathbf{x}}_F^\beta$ from the remaining subblocks by

$$\tilde{\mathbf{y}}_F = \tilde{\mathbf{y}}_F - \bar{\mathbf{G}}_\beta \hat{\mathbf{x}}_F^\beta \qquad (46)$$

where $\bar{\mathbf{G}}_\beta = \tilde{\mathbf{G}}(1 : N_{av}, n\beta - n + 1 : n\beta)$. In other words, after the detection of $\tilde{\mathbf{x}}_F^\beta$, its effect on the received signal vector is totally eliminated by the update equation given by (46) under the assumption that $\hat{\mathbf{x}}_F^\beta = \tilde{\mathbf{x}}_F^\beta$.

4) SP Detector: The signal-power (SP) detector for the OFDM-IM scheme applies the same detection and cancelation techniques as the block cancellation detector; however, first, it calculates the SP values for all subblocks via

$$SP_\beta = \left\| \tilde{\mathbf{G}}_\beta \right\|_F^2 \qquad (47)$$

and then sorts these SP values, starting from the subblock with the highest SP, and proceeding towards the subblock with the lowest SP. In other words, the SP detector starts with the detection of the subblock with the highest SP; after the detection of this subblock, it updates the received signal vector using (46) and so on.

VI. SIMULATION RESULTS

In this section, we present simulation results for the OFDM-IM scheme with different configurations and make comparisons with classical OFDM, ESIM-OFDM [14] and the ICI self-cancellation OFDM scheme [25]. The BER performance of these schemes was evaluated via Monte Carlo simulations. In what follows, we investigate the error performance of OFDM-IM under ideal and realistic channel conditions.

A. Performance of OFDM-IM Under Ideal Channel Conditions

In this subsection, we investigate the error performance of OFDM-IM in the presence of frequency selective channels only as described in Section II. In all simulations, we assumed the following system parameters: $N = 128$, $\nu = 10$ and $L = 16$.

In Fig. 2, we compare the BER performance of the ML, the reduced-complexity ML and the LLR detectors for OFDM-IM with the same system parameters for BPSK. As seen from the left hand side of Fig. 2, for the $n = 4$, $k = 2$ scheme, the ML and reduced-complexity ML decoders exhibit exactly the same BER performance, as expected. As mentioned previously, the
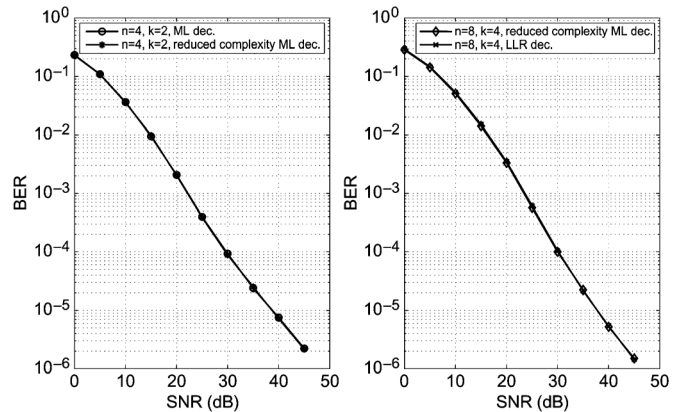

Fig. 2. Comparison of ML, reduced-complexity ML and LLR detectors for OFDM-IM with different configurations.

reduced-complexity ML decoder calculates the corresponding LLR sum values for each possible index combination from the predefined look-up table and then decides on the most likely combination. On the right hand side of Fig. 2, we compared the BER performance of two completely different $n = 8$, $k = 4$ OFDM-IM schemes. The $n = 8$, $k = 4$ scheme, which uses a reduced complexity ML decoder, employs a look-up table of size 64, composed of lexicographically ordered 4 combinations of 8. On the other hand, the $n = 8$, $k = 4$ scheme with an LLR decoder, does not employ a look-up table, instead it uses the combinatorial method. As seen from Fig. 2, interestingly, the LLR detector, which is actually a near-ML detector, achieves the same BER performance as that of the ML detector. This can be attributed to the fact that the percentage of the number of unused combinations ($C(n, k) - c = 70 - 64 = 6$) out of the all possible index combinations ($C(n, k) = 70$) is relatively low for $n = 8$, $k = 4$ selection (8.6%). Therefore, we conclude that it is not very likely for the receiver to decide to a catastrophic set of active indices for this case. On the other hand, this percentage is equal to 36.3% and 10.7% for $n = 16$, $k = 8$ and $n = 32$, $k = 16$ OFDM-IM schemes respectively. Note that, it is not possible to implement a look-up table, therefore an ML decoder, for these schemes to make comparisons.

In Fig. 3, we compared the BER performance of different OFDM-IM schemes with classical OFDM for BPSK. As seen from Fig. 3, at a BER value of 10^{-5} our new scheme with $n = 4$, $k = 2$ achieves approximately 6 dB better BER performance than classical OFDM operating at the same spectral efficiency. This significant improvement in BER performance can be explained by the improved distance spectrum of the OFDM-IM scheme, where higher diversity orders are obtained for the bits carried by the active indices. For comparison, the theoretical curve obtained from (32) is also depicted on the same figure for the $n = 4$, $k = 2$ scheme, which uses an ML decoder. As seen from Fig. 3, the theoretical curve becomes very tight with the computer simulation curve as the SNR increases. For higher values of n, we employ the combinatorial method for the index mapping and demapping operations with the LLR decoder. We observe that despite their increased data rates, the OFDM-IM schemes with $n = 8$, $k = 4$ and $n = 32$, $k = 16$, exhibit BER
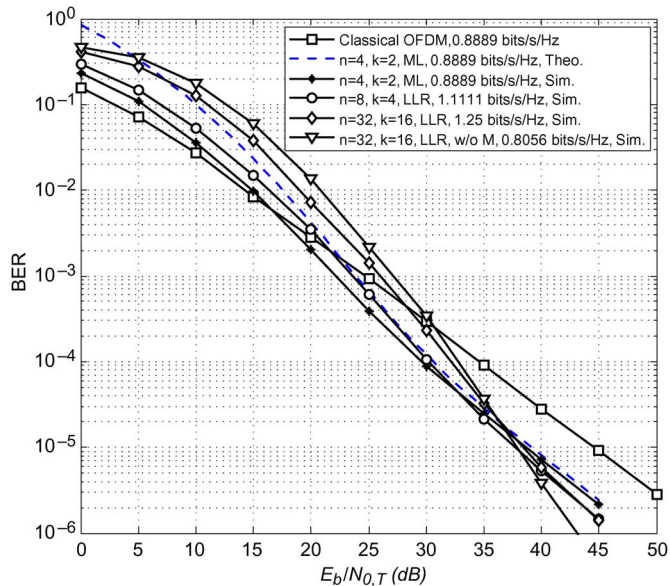
Fig. 3. BER performance of OFDM-IM with different configurations, BPSK.

Fig. 4. The effect of varying ν values on BER performance for $n = 4, k = 2$ and $n = 32, k = 16$ OFDM-IM schemes.

performance close to the low-rate $n = 4, k = 2$ OFDM scheme. This can be explained by the fact that for high SNR, the error performance of the OFDM-IM scheme is dominated by the PEP events with $r = 1$ as we discussed in the Section IV. Finally we observe from Fig. 3 that OFDM-IM achieves significantly better BER performance than classical OFDM at high SNR values due to the improved error performance of the bits transmitted in the index domain, which is more effective at high SNR.

In Fig. 3, we also show the BER performance of the OFDM-IM scheme which does not employ M-ary modulation ($n = 32, k = 16$, LLR, w/o M), and relies on the transmission of data via subcarrier indices only. As seen from Fig. 3, this scheme achieves a diversity order of two, as proved in Section IV, and exhibits the best BER performance for high SNR values with a slight decrease in the spectral efficiency compared to classical OFDM employing BPSK modulation.

In Fig. 4, we investigate the effect of varying fading channel tap lengths on the error performance of the OFDM-IM schemes using BPSK with $n = 4, k = 2$ and $n = 32, k = 16$ in the light of our analysis presented in Remark 2 of Section IV. As seen from this figure, increasing ν values create a separation in BER performance especially in the mid SNR region, while the differences in error performance curves become smaller in the high SNR region as expected, due to the identical worst case PEP events. On the other hand, we observe that increasing ν values have a bigger effect on the BER performance for the $n = 32, k = 16$ scheme due to the larger variation in r_1 values of Table II for this configuration.

In Figs. 5–7, we compare the BER performance of the proposed scheme with classical OFDM and ESIM-OFDM for three different spectral efficiency values (0.8889, 1.7778 and 2.6667 bits/s/Hz, respectively). We consider ML and LLR detectors for ESIM-OFDM and OFDM-IM, respectively. As seen from Figs. 5–7, the proposed scheme provides significant improvements in error performance compared to ESIM-OFDM and OFDM operating at the same spectral efficiency. Furthermore, we observe that ESIM-OFDM cannot provide
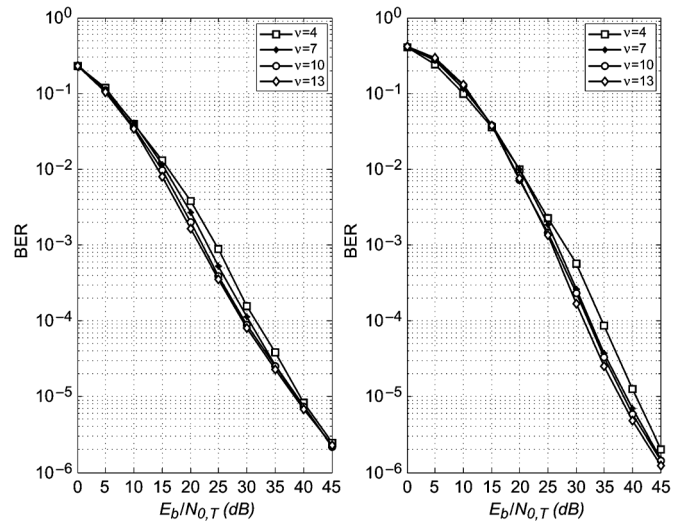
noticeable performance improvement over classical OFDM when both schemes operate at the same spectral efficiency since ESIM-OFDM requires higher order modulation.

B. Performance of OFDM-IM Under Channel Estimation Errors

In Fig. 8, we present computer simulation results for the imperfect CSI case. As a reference, we consider the BER performance of the $n = 4, k = 2$ OFDM-IM scheme using BPSK for $Q = 1$. In Fig. 8, the theoretical upper bound calculated from (41) is also given. For comparison, as mentioned in Section V-A, we also present the theoretical curve obtained by the calculation of the UPEP values, considering only the worst case error events. As seen from Fig. 8, both approximations become very tight with increasing SNR values and can be used to predict the BER behavior of the OFDM-IM scheme under channel estimation errors.

C. Performance of OFDM-IM Under Mobility Conditions

In this subsection, we present computer simulation results for the OFDM-IM scheme operating under realistic channel mobility conditions. Our simulation parameters are given in Table III. A multipath wireless channel having an exponentially decaying power delay profile with the normalized powers is assumed [26].

In Fig. 9, we compare the BER performance of three different OFDM-IM schemes employing various detectors with the classical OFDM and the ICI self-cancellation OFDM scheme proposed in [25] for a mobile terminal moving at a speed of $v = 100 \, \text{km/h}$. OFDM and OFDM-IM schemes use BPSK while the ICI self-cancellation scheme uses QPSK and applies precoding. For the $n = 4, k = 2$ OFDM-IM scheme, four different type of detectors presented in Section V-B are used. For the higher rate $n = 8, k = 4$ and $n = 22, k = 11$ OFDM-IM schemes, which rely on the combinatorial method to determine the active indices, the received signal vector is processed by the MMSE detector and then an LLR detector is employed. On the other hand, the classical OFDM scheme and ICI self-cancellation OFDM
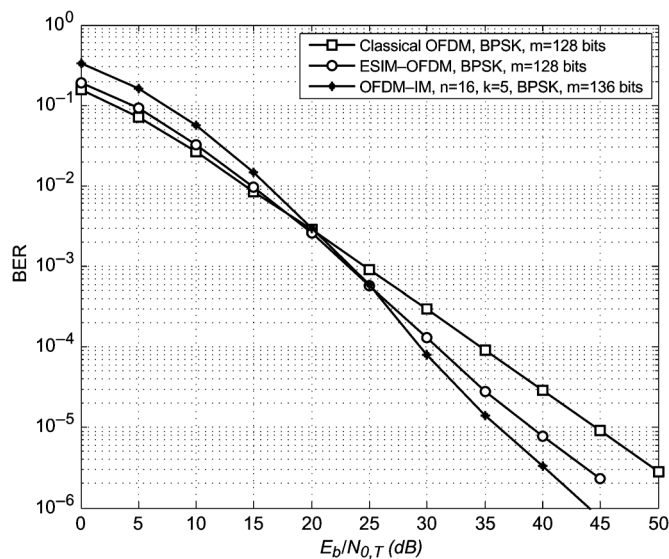
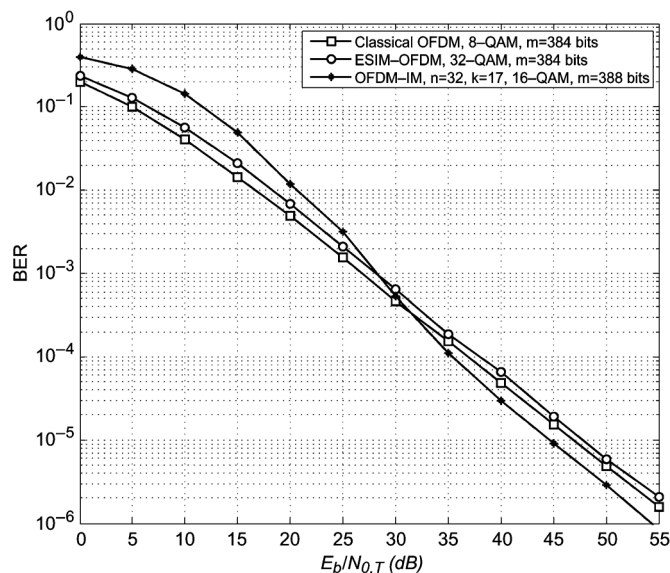Fig. 5. Performance of classical OFDM, ESIM-OFDM and OFDM-IM for 0.8889 bits/s/Hz.

Fig. 7. Performance of classical OFDM, ESIM-OFDM and OFDM-IM for 2.6667 bits/s/Hz.
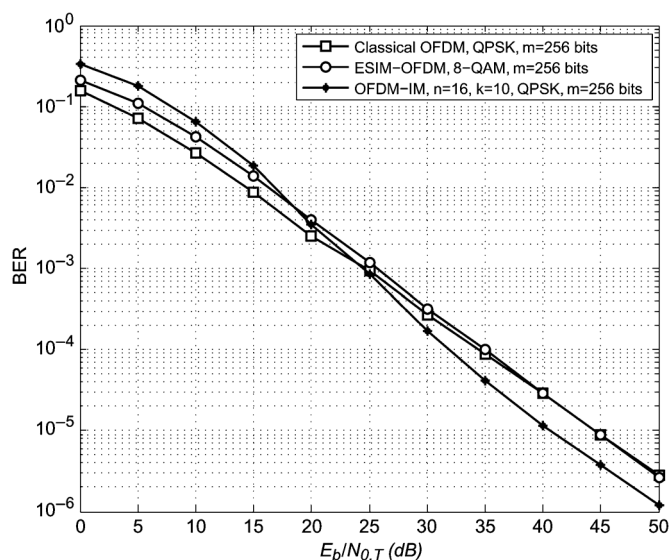

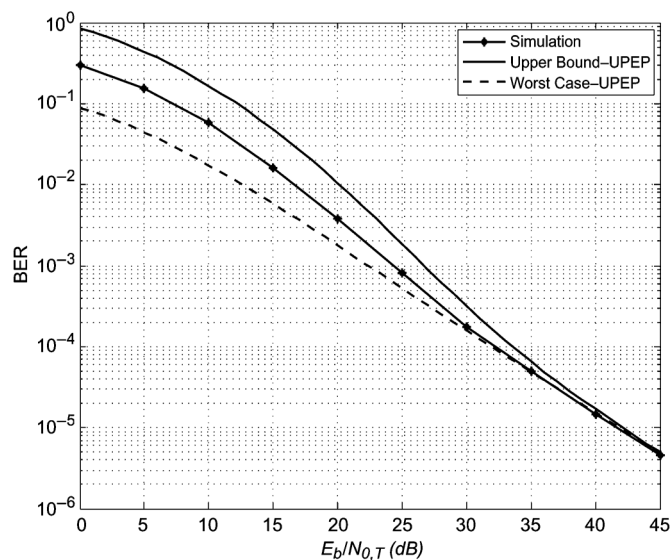Fig. 6. Performance of classical OFDM, ESIM-OFDM and OFDM-IM for 1.7778 bits/s/Hz.

Fig. 8. BER performance of the $n = 4$, $k = 2$ OFDM-IM scheme with imperfect CSI, BPSK, $Q = 1$.

scheme employ an MMSE detector. As seen from Fig. 9, compared to classical OFDM, OFDM-IM cannot exhibit exceptional performance with the MMSE detector, since this detector, which works as an equalizer, does not improve the detection process of the OFDM-IM scheme, which relies on the fluctuations between the channel coefficients to determine the indices of the active subcarriers. In other words, the MMSE equalizer eliminates the effect of the channel coefficients, and therefore, the receiver makes decisions by simply calculating the Euclidean distance between the constellation points and the received signal. On the other hand, the interference unaware submatrix receiver tends to error floor just after reaching to the BER value of 10^{-5}. This can be explained by the fact that this detector does not take into account the inference between different subblocks; therefore, the performance is limited by this interference with increasing SNR

TABLE III
SIMULATION PARAMETERS

Channel Bandwidth	1.5 MHz
Number of Subcarriers (N)	128
Number of Occuppied Subcarriers	88
Subcarrier Spacing	15 kHz
Sampling Frequency	1.92 MHz
Carrier Frequency (f_c)	2.5 GHz
Number of Multipaths (ν)	10
Cyclic Prefix Length (L)	10
Velocity (v)	100, 300 km/h

values, which causes an error floor. Although considering the interference, the performance of the block cancellation detector is also dominated by the error floor as seen from Fig. 9; however, it pulls downs the error floor to lower BER values compared to the submatrix receiver. Meanwhile the SP detector provides
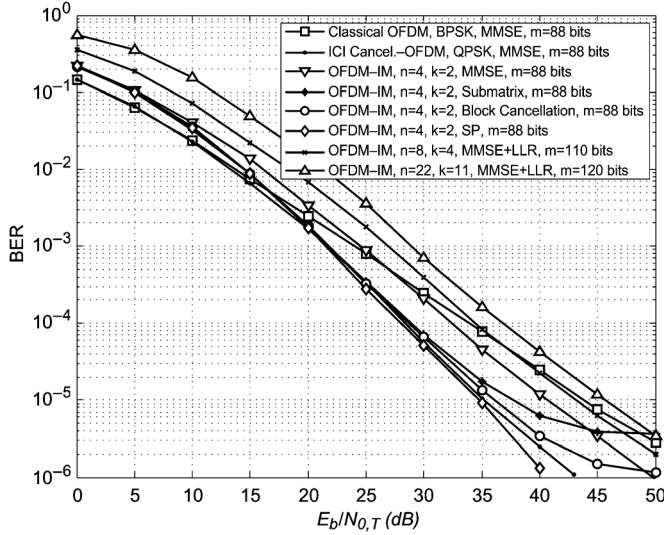
Fig. 9. Performance of OFDM-IM for a mobile terminal moving at a speed of $v = 100$ km/h, BPSK.
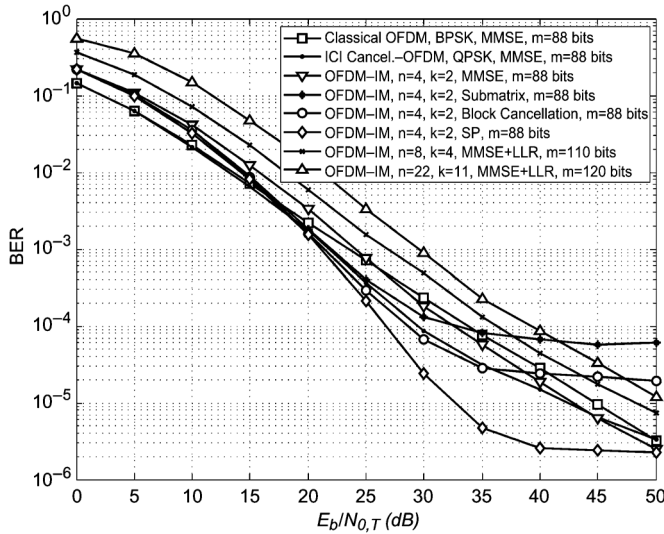

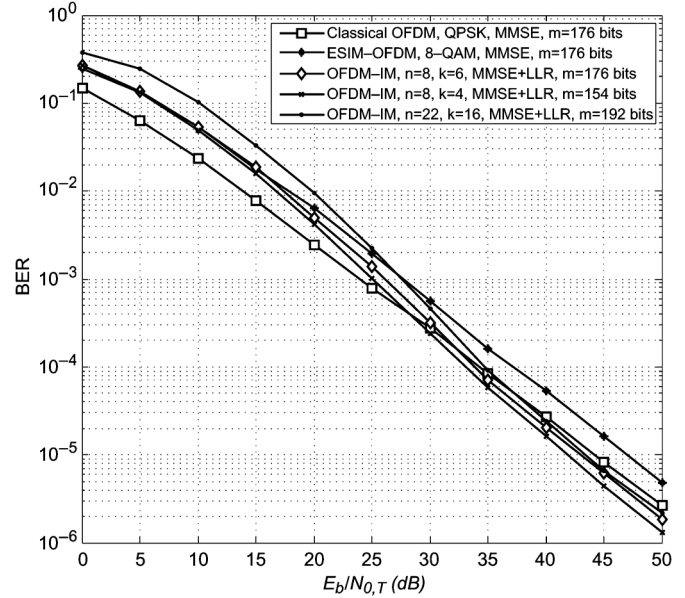Fig. 10. Performance of OFDM-IM for a mobile terminal moving at a speed of $v = 300$ km/h, BPSK.

Fig. 11. Performance of OFDM-IM for a mobile terminal moving at a speed of $v = 100$ km/h, QPSK.

We observe from Fig. 10 that the OFDM-IM scheme with the SP detector provides a significant improvement (around 12 dB) compared to classical OFDM if the target BER is 10^{-5}, while for much lower target BER values, one may consider the OFDM-IM scheme with the MMSE detector, which is invulnerable to the error floor.

In Fig. 11, we compare the BER performance of OFDM-IM using QPSK and employing the MMSE and LLR detector with classical OFDM using QPSK and ESIM-OFDM using 8-QAM for a mobile terminal moving at a speed of $v = 100$ km/h. As seen from Fig. 11, for the same spectral efficiency, the proposed scheme achieves better BER performance than the classical OFDM and ESIM-OFDM, while the higher rate $n = 22$, $k = 16$ OFDM-IM scheme achieves better BER performance than classical OFDM with increasing SNR.

D. Complexity Comparisons

In this subsection, we compare the computational complexity of the proposed method with the reference systems. Without mobility, the detection complexity (in terms of complex operations) of the LLR and the reduced-complexity ML detectors employed in the proposed scheme is the same as that of the classical OFDM and ESIM-OFDM systems, and, as shown in Sections II and III, it is $\sim \mathcal{O}(M)$ per subcarrier. On the other hand, in the case of high mobility, while the detection complexity of the MMSE+LLR detector of the proposed scheme is the same as the classical OFDM, ESIM-OFDM and ICI self-cancelation OFDM schemes $(\sim \mathcal{O}(M))$, the detection complexity of the ML based detectors (submatrix, block cancelation and SP detectors) of the proposed scheme grows exponentially with increasing values of k, as shown in Section V, i.e., it is $\sim \mathcal{O}(M^k)$ per subblock, which is higher than the reference systems. Consequently, this detector can be used only for smaller values of k, such as $k = 2$. On the other hand, for higher values of k, the MMSE+LLR detector is the potential technique to employ in practice.

the best error performance by completely eliminating the error floor in the considered BER regime. For a BER value of 10^{-5}, the SP detector provides approximately 9 dB better BER performance than classical OFDM. We also observe that the proposed scheme with the SP detector achieves better BER performance than the ICI self-cancellation OFDM scheme at high SNR. In the same figure, we also show the BER curves of higher rate $n = 8$, $k = 4$ and $n = 22$, $k = 11$ OFDM-IM schemes. Interestingly, our $n = 8$, $k = 4$ OFDM-IM scheme achieves better BER performance than classical OFDM with increasing SNR values even if transmitting 22 additional bits per OFDM block.

In Fig. 10, we extend our simulations to the $v = 300$ km/h case. As seen from Fig. 10, by increasing the mobile terminal velocity, the detectors that do not use the MMSE equalization, tend to have error floors for lower BER values compared to the $v = 100$ km/h case, and the ICI self-cancellation OFDM scheme cannot compete with the proposed scheme any more.

VII. CONCLUSION AND FUTURE WORK

A novel multicarrier scheme called OFDM with index modulation, which uses the indices of the active subcarriers to transmit data, has been proposed in this paper. In this scheme, inspired by the recently proposed SM concept, the incoming information bits are transmitted in a unique fashion to improve the error performance as well as to increase spectral efficiency. Different transceiver structures are presented for the proposed scheme which operates on frequency selective fading channels with or without terminal mobility. It has been shown that the proposed scheme achieves significantly better BER performance than classical OFDM under different channel conditions. The following points remain unsolved in this work: i) the error performance analysis of OFDM-IM under channel estimation errors for general M-ary signal constellations and for the high mobility case; ii) the error performance analysis of the LLR and MMSE detectors of the OFDM-IM scheme; and iii) the optimal selection method of n and k values for a given bit rate.

As the proposed scheme works well for the uplink system, for the downlink system it can be integrated into orthogonal frequency division multiple access (OFDMA) systems as well. In an OFDMA system, after allocating the available subcarriers to different users, each user can apply OFDM-IM for its subcarriers. Therefore, in general, for U users, U different OFDM-IM schemes can be incorporated operating simultaneously to create the overall OFDMA system. Note that the OFDM-IM scheme provides coding gain compared to classical OFDM. In order to obtain additional diversity gain, it can be combined by linear constellation precoding (LCP) proposed in [27]; however, this is beyond the scope of this paper and is a potential future research topic.

REFERENCES

[1] H. Şenol, E. Panayırcı, and H. V. Poor, "Nondata-aided joint channel estimation and equalization for OFDM systems in very rapidly varying mobile channels," *IEEE Trans. Signal Process.*, vol. 60, no. 8, pp. 4236–4253, Aug. 2012.

[2] E. Panayırcı, H. Şenol, and H. V. Poor, "Joint channel estimation, equalization, and data detection for OFDM systems in the presence of very high mobility," *IEEE Trans. Signal Process.*, vol. 58, no. 8, pp. 4225–4238, Aug. 2010.

[3] R. Mesleh, H. Haas, S. Sinanovic, C. W. Ahn, and S. Yun, "Spatial modulation," *IEEE Trans. Veh. Technol.*, vol. 57, no. 4, pp. 2228–2241, Jul. 2008.

[4] J. Jeganathan, A. Ghrayeb, and L. Szczecinski, "Spatial modulation: Optimal detection and performance analysis," *IEEE Commun. Lett.*, vol. 12, no. 8, pp. 545–547, Aug. 2008.

[5] E. Başar, Ü. Aygölü, E. Panayırcı, and H. V. Poor, "Space-time block coded spatial modulation," *IEEE Trans. Commun.*, vol. 59, no. 3, pp. 823–832, Mar. 2011.

[6] J. Jeganathan, A. Ghrayeb, L. Szczecinski, and A. Ceron, "Space shift keying modulation for MIMO channels," *IEEE Trans. Wireless Commun.*, vol. 8, no. 7, pp. 3692–3703, Jul. 2009.

[7] E. Başar, Ü. Aygölü, E. Panayırcı, and H. V. Poor, "New trellis code design for spatial modulation," *IEEE Trans. Wireless Commun.*, vol. 10, no. 9, pp. 2670–2680, Aug. 2011.

[8] S. Sugiura, S. Chen, and L. Hanzo, "Coherent and differential space-time shift keying: A dispersion matrix approach," *IEEE Trans. Commun.*, vol. 58, no. 11, pp. 3219–3230, Nov. 2010.

[9] J. Jeganathan, A. Ghrayeb, and L. Szczecinski, "Generalized space shift keying modulation for MIMO channels," in *Proc. IEEE Int. Symp. Personal, Indoor, Mobile Radio Commun.*, Sep. 2008, pp. 1–5.

[10] J. Fu, C. Hou, W. Xiang, L. Yan, and Y. Hou, "Generalised spatial modulation with multiple active transmit antennas," in *Proc. IEEE GLOBECOM Workshops*, Dec. 2010, pp. 839–844.

[11] E. Başar, Ü. Aygölü, E. Panayırcı, and H. V. Poor, "Performance of spatial modulation in the presence of channel estimation errors," *IEEE Commun. Lett.*, vol. 16, no. 2, pp. 176–179, Feb. 2012.

[12] E. Başar, Ü. Aygölü, E. Panayırcı, and H. V. Poor, "Super-orthogonal trellis-coded spatial modulation," *IET Commun.*, vol. 6, no. 17, pp. 2922–2932, Nov. 2012.

[13] R. Abu-alhiga and H. Haas, "Subcarrier-index modulation OFDM," in *Proc. IEEE Int. Sym. Personal, Indoor, Mobile Radio Commun.*, Tokyo, Japan, Sep. 2009, pp. 177–181.

[14] D. Tsonev, S. Sinanovic, and H. Haas, "Enhanced subcarrier index modulation (SIM) OFDM," in *Proc. IEEE GLOBECOM Workshops*, Dec. 2011, pp. 728–732.

[15] P. Robertson, E. Villebrun, and P. Hoeher, "A comparison of optimal and sub-optimal MAP decoding algorithms operating in the log domain," in *Proc. IEEE Int. Conf. Commun.*, Seattle, WA, USA, Jun. 1995, pp. 1009–1013.

[16] D. E. Knuth, *The Art of Computer Programming*. Reading, MA, USA: Addison-Wesley, 2005, vol. 4, ch. 7.2.1.3, Fascicle 3.

[17] J. D. McCaffrey, "Generating the mth lexicographical element of a mathematical combination," *MSDN Library*, Jul. 2004 [Online]. Available: http://msdn.microsoft.com/en-us/library/aa289166(VS.71).aspx

[18] H. Jafarkhani, *Space-Time Coding*. Cambridge, UK: Cambridge Univ. Press, 2005.

[19] M. Chiani and D. Dardari, "Improved exponential bounds and approximation for the Q-function with application to average error probability computation," in *Proc. IEEE Global Telecommun. Conf.*, Bologna, Italy, 2002, vol. 2, pp. 1399–1402.

[20] R. A. Horn and C. R. Johnson, *Matrix Analysis*. Cambridge, U.K.: Cambridge Univ. Press, 1985.

[21] B. Wang and F. Zhang, "Some inequalities for the eigenvalues of the product of positive semidefinite Hermitian matrices," *Linear Algebra Its Appl.*, vol. 160, pp. 113–118, 1992.

[22] V. Tarokh, A. Naguib, N. Seshadri, and A. Calderbank, "Space-time codes for high data rate wireless communication: Performance criteria in the presence of channel estimation errors, mobility, and multiple paths," *IEEE Trans. Commun.*, vol. 47, no. 2, pp. 199–207, Feb. 1999.

[23] N. R. Goodman, "Statistical analysis based on a certain multivariate complex Gaussian distribution (an introduction)," *Ann. Math. Stat.*, vol. 34, no. 1, pp. 152–177, May 1963.

[24] E. Panayırcı, H. Doğan, and H. V. Poor, "Low-complexity MAP-based successive data detection for coded OFDM systems over highly mobile wireless channels," *IEEE Trans. Veh. Technol.*, vol. 60, no. 6, pp. 2849–2857, Jul. 2011.

[25] Y. Zhao and S. G. Haggman, "Intercarrier interference self-cancellation scheme for OFDM mobile communication systems," *IEEE Trans. Commun.*, vol. 49, no. 7, pp. 1185–1191, Jul. 2001.

[26] Y.-S. Choi, P. Voltz, and F. Cassara, "On channel estimation and detection for multicarrier signals in fast and selective Rayleigh fading channels," *IEEE Trans. Commun.*, vol. 49, no. 8, pp. 1375–1387, Aug. 2001.

[27] Z. Liu, Y. Xin, and G. B. Giannakis, "Linear constellation precoding for OFDM with maximum multipath diversity and coding gains," *IEEE Trans. Commun.*, vol. 51, no. 3, pp. 1185–1191, Jun. 2001.

Ertuğrul Başar (S'09–M'13) was born in Istanbul, Turkey, in 1985. He received the B.S. degree from Istanbul University, Istanbul, Turkey, in 2007, and the M.S. and Ph.D degrees from the Istanbul Technical University, Istanbul, Turkey, in 2009 and 2013, respectively. Dr. Başar spent the academic year 2011–2012, in the Department of Electrical Engineering, Princeton University, New Jersey, USA. Currently, he is a research assistant at Istanbul Technical University. His primary research interests include MIMO systems, space-time coding, spatial modulation systems, OFDM and cooperative diversity.
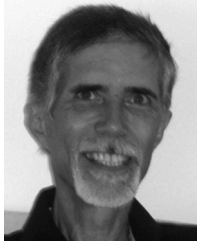
Ümit Aygölü (M'90) received his B.S., M.S. and Ph.D. degrees, all in electrical engineering, from Istanbul Technical University, Istanbul, Turkey, in 1978, 1984 and 1989, respectively. He was a Research Assistant from 1980 to 1986 and a Lecturer from 1986 to 1989 at Yildiz Technical University, Istanbul, Turkey. In 1989, he became an Assistant Professor at Istanbul Technical University, where he became an Associate Professor and Professor, in 1992 and 1999, respectively. His current research interests include the theory and applications of combined channel coding and modulation techniques, MIMO systems, space-time coding and cooperative communication.

Erdal Panayırcı (S'73–M'80–SM'91–F'03) received the Diploma Engineering degree in Electrical Engineering from Istanbul Technical University, Istanbul, Turkey and the Ph.D. degree in Electrical Engineering and System Science from Michigan State University, USA. Until 1998 he has been with the Faculty of Electrical and Electronics Engineering at the Istanbul Technical University, where he was a Professor and Head of the Telecommunications Chair. Currently, he is Professor of Electrical Engineering and Head of the Electronics Engineering Department at Kadir Has University, Istanbul, Turkey. Dr. Panayırcı's recent research interests include communication theory, synchronization, advanced signal processing techniques and their applications to wireless communications, coded modulation and interference cancelation with array processing. He published extensively in leading scientific journals and international conferences. He has co-authored the book *Principles of Integrated Maritime Surveillance Systems* (Boston, Kluwer Academic Publishers, 2000).

Dr. Panayırcı spent the academic year 2008–2009, in the Department of Electrical Engineering, Princeton University, New Jersey, USA. He has been the principal coordinator of a 6th and 7th Frame European project called NEWCOM (Network of Excellent on Wireless Communications) and WIMAGIC Strep project representing Kadir Has University. Dr. Panayırcı was an Editor for IEEE TRANSACTIONS ON COMMUNICATIONS in the areas of Synchronization and Equalizations in 1995–1999. He served as a Member of IEEE Fellow Committee in 2005–2008. He was the Technical Program Chair of ICC-2006 and PIMRC-2010 both held in Istanbul, Turkey. Presently he is head of the Turkish Scientific Commission on Signals and Systems of URSI (International Union of Radio Science).

H. Vincent Poor (S'72–M'77–SM'82–F'87) received the Ph.D. degree in EECS from Princeton University in 1977. From 1977 until 1990, he was on the faculty of the University of Illinois at Urbana-Champaign. Since 1990 he has been on the faculty at Princeton, where he is the Michael Henry Strater University Professor of Electrical Engineering and Dean of the School of Engineering and Applied Science. Dr. Poor's research interests are in the areas of stochastic analysis, statistical signal processing, and information theory, and their applications in wireless networks and related fields such as social networks and smart grid. Among his publications in these areas the recent books *Smart Grid Communications and Networking* (Cambridge, 2012) and *Principles of Cognitive Radio* (Cambridge, 2013).

Dr. Poor is a member of the National Academy of Engineering and the National Academy of Sciences, a Fellow of the American Academy of Arts and Sciences, an International Fellow of the Royal Academy of Engineering (U.K.), and a Corresponding Fellow of the Royal Society of Edinburgh. He is also a Fellow of the Institute of Mathematical Statistics, the Acoustical Society of America, and other organizations. He received the Technical Achievement and Society Awards of the SPS in 2007 and 2011, respectively. Recent recognition of his work includes the 2010 IET Ambrose Fleming Medal, the 2011 IEEE Eric E. Sumner Award, and honorary doctorates from Aalborg University, the Hong Kong University of Science and Technology, and the University of Edinburgh.